

## Original article

# A Comparative Study of $^{68}\text{Ga}$ Gallium-Prostate Specific Membrane Antigen Positron Emission Tomography-Computed Tomography and Magnetic Resonance Imaging for Lymph Node Staging in High Risk Prostate Cancer Patients: An Initial Experience

Manoj Gupta, Partha S. Choudhury, Dibyamohan Hazarika<sup>1</sup>, Sudhir Rawal<sup>2</sup>

Departments of Nuclear Medicine, <sup>1</sup>Radiology and <sup>2</sup>Uro Oncology, Rajiv Gandhi Cancer Institute and Research Centre, New Delhi, India

## Abstract

Lymph node staging plays an important role in planning initial management in nonmetastatic prostate cancer. This article compares the role of  $^{68}\text{Ga}$  Gallium ( $^{68}\text{Ga}$ )-prostate specific membrane antigen (PSMA) positron emission tomography-computed tomography (PET-CT) with magnetic resonance imaging (MRI), which is considered the standard staging modality. Out of 39 high-risk prostate cancer patients who underwent  $^{68}\text{Ga}$ -PSMA PET-CT for staging (December 2014–December 2015), 12 patients underwent radical prostatectomy along with ePLND and were included in the analysis. Findings of the PSMA PET and MRI were compared with final histopathology. Sensitivity, specificity, positive predictive value (PPV), negative predictive value (NPV), and accuracy of  $^{68}\text{Ga}$ -PSMA PET-CT and MRI were calculated for numbers of patients and pelvic lymph node metastasis. Chi-square test, McNemar's test, and receiver operating characteristic (ROC) analysis were also done.  $^{68}\text{Ga}$ -PSMA PET-CT and MRI sensitivity, specificity, PPV, NPV, and accuracy for number of patients detection were 100%, 80%, 87.5%, 100%, 91.67%, and 57.14%, 80%, 80%, 57.4%, 66.67%, respectively. For detection of metastatic lymph node, it was 66.67%, 98.61%, 85.71%, 95.95%, 95.06% and 25.93%, 98.61%, 70%, 91.42%, 90.53%, respectively. Difference of lymph nodal detectability was statistically significant on Chi-square test. On McNemar's test, *P* value was statistically insignificant for number of patient detection (*P* = 0.250) but statistically significant for lymph nodal detection (*P* = 0.001) for  $^{68}\text{Ga}$ -PSMA PET-CT. In ROC analysis, area under the curve was also significantly high for lymph node detectability by  $^{68}\text{Ga}$ -PSMA PET-CT. Our initial experience shows that  $^{68}\text{Ga}$ PSMA PET-CT is a very promising tracer for N staging in the initial workup of prostate cancer. It has the potential to impact patient's initial management and can up- and down-stage effectively.

**Keywords:**  $^{68}\text{Ga}$  Gallium-prostate specific membrane antigen positron emission tomography-computed tomography, high-risk prostate cancer, magnetic resonance imaging, pelvic lymph node comparison

## Address for correspondence:

Dr. Manoj Gupta, Department of Nuclear Medicine,  
Rajiv Gandhi Cancer Institute and Research Centre,  
Sector 5, Rohini, New Delhi - 110 085, India.  
E-mail: docmanojgupta@yahoo.com

## Introduction

Prostate cancer is the second most common cancer and sixth leading cause of cancer death in man

This is an open access article distributed under the terms of the Creative Commons Attribution-NonCommercial-ShareAlike 3.0 License, which allows others to remix, tweak, and build upon the work non-commercially, as long as the author is credited and the new creations are licensed under the identical terms.

**For reprints contact:** reprints@medknow.com

**How to cite this article:** Gupta M, Choudhury PS, Hazarika D, Rawal S. A comparative study of  $^{68}\text{Ga}$  Gallium-prostate specific membrane antigen positron emission tomography-computed tomography and magnetic resonance imaging for lymph node staging in high risk prostate cancer patients: An initial experience. World J Nucl Med 2017;16:186-91.

## Access this article online

### Quick Response Code:



### Website:

www.wjnm.org

### DOI:

10.4103/1450-1147.207272

worldwide.<sup>[1]</sup> In addition to the tumor-node-metastasis staging, serum prostate specific antigen (PSA), and Gleason score are also an integral part of staging and treatment determinants.<sup>[2,3]</sup> Nomograms are available to predict the risk of distant and nodal metastasis which substitute the nodal staging procedure in low risk (PSA <10 µg/L, Gleason 6 or less, and stage T2a or less) patients.<sup>[4-6]</sup> However, in a patient with high risk of metastatic disease (PSA >20 µg/L, Gleason 8 or more, and stage T3 or more), a suitable staging procedure may be beneficial before a potentially curative treatment is planned. Current published literature indicates that computed tomography (CT) and magnetic resonance imaging (MRI) perform similarly in the detection of pelvic lymph node metastasis.<sup>[7]</sup> In either case, the lymph nodal involvement criteria solely based on the size and shape. A threshold of 1 cm in the short axis for the oval lymph node and 0.8 cm for the round lymph node has been a recommended criteria for abnormal lymph node in morphological imaging despite the fact that a significant number of metastatic lymph nodes can be sub-cm in size.<sup>[8]</sup> To overcome these limitations, functional imaging techniques using radiopharmaceuticals and targets have been recently identified.<sup>[9]</sup> Prostate specific membrane antigen (PSMA) is the preferred one among these targets. PSMA is overexpressed in the prostate cancer cell, and it has a positive correlation with the grade of tumor.<sup>[10,11]</sup> Glu-NH-CO-NH-Lys-(Axe)-(68Gallium [68Ga]-[HBED-CC]) positron emission tomography-CT (PET-CT) has recently showed promising results in suspected recurrence of prostate cancer.<sup>[12,13]</sup> We analyzed our retrospective data prospectively to see the lymph node detection capability of 68Ga-PSMA PET-CT in comparison to MRI in high-risk prostate cancer during staging. To the best of our understanding, we were not aware of any similar studies in the literature.

## Materials and Methods

A total of 39 high risk (PSA >20 µg/L, Gleason 8 or more, and stage T3 or more) prostate cancer patients underwent 68Ga-PSMA PET-CT between December 2014 and December 2015. Twenty patients (51.3%) had distant metastasis, five (12.8%) were planned for radiotherapy, and two (5.1%) had high intensity focused ultrasound and underwent their treatments accordingly. We included 12 patients who were planned and underwent radical prostatectomy with ePLND based on the findings of the imaging in the final analysis. The findings were correlated with final histopathology (HPE), which was taken as the gold standard.

A 1.11 GBq iTG self-shielded Ga-68 generator provided metal-free 68Ga chloride ready for peptide labeling following elution with 4 ml of 0.05 N HCl. The entire synthesis was performed in-house in a laminar flow

cabinet with PSMA peptide GMP kits from ABx using an IQS-fluidic labeling module (iTG) that did not require computer control.

## Imaging protocol

Standard 68Ga-PSMA PET-CT imaging protocol was followed. After 4 h of fasting and maintaining proper hydration, 2 MBq/kg body weight of 68Ga-PSMA was injected intravenously. Water was used as negative oral contrast. After approximately 60 min, whole body scan (vertex to mid-thigh) was performed on a dedicated full-ring hybrid PET-CT system (Biograph TruePoint40 with LSO crystal from Siemens Healthcare) with 4 min per bed position in three-dimensional mode. A low-dose CT scan (40 mAs and 120 kVp) was used for attenuation correction and localization. Noncontrast MRI of the pelvis was performed in Siemens 1.5 Tesla Avanto System using body matrix coil and T1W SE, T2W turbo spin echo, and short-tau inversion recovery sequence in axial, coronal, and sagittal planes. High-resolution small field of view T2 images without fat saturation were obtained for local anatomical delineation. Diffusion-weighted images were obtained with B values of 500 and 1000 s/mm<sup>2</sup>, and ADC maps were generated.

## Image interpretation

68Ga-PSMA PET-CT scan was reinterpreted independently by two nuclear medicine physician without access to MRI or HPE findings. Unambiguously increased PSMA uptake other than physiological distribution in a comparison to background was taken as positive. No size criterion was used for PET interpretation. MRI reported independently by the radiologist was taken into analysis. Lymph node which is equal to or more than 1 cm in the smallest diameter was considered abnormal. Right and left pelvic lymph nodes were separately recorded for both imaging modalities.

## Results

Patient's data are summarized in Table 1. Of total, 243 lymph nodes were pathologically sampled in 12 patients (average 20.25 and median twenty lymph nodes per patient). Seven (58.33%) patients with total 27 (11.11%) lymph nodes were positive on HPE. 68Ga-PSMA PET-CT and MRI were positive in eight patients and five patients, respectively. Their diagnostic value for number of patient with at least one positive lymph node on HPE is given in Tables 2 and 3, respectively.

68Ga-PSMA PET-CT and MRI diagnostic sensitivity, specificity, positive predicative value (PPV), negative predicative value (NPV), and accuracy for detection of number of patients with at one positive lymph node on HPE were 100%, 80%, 87.5%, 100%, 91.67%, and 57.14%, 80%, 80%, 57.4%, 66.67%, respectively.

**Table 1: Patients demography with magnetic resonance imaging, <sup>68</sup>Gallium-prostate specific membrane antigen-positron emission tomography-computed tomography, and histopathological findings**

| Age Gleason's PSA µg/L<br>score |     |        | Lymph node involvement |              |             |       |              |             |               |                |              |             |
|---------------------------------|-----|--------|------------------------|--------------|-------------|-------|--------------|-------------|---------------|----------------|--------------|-------------|
|                                 |     |        | MRI                    |              |             | PSMA  |              |             | HPE           |                |              |             |
|                                 |     |        | Total                  | Right pelvic | Left pelvis | Total | Right pelvic | Left pelvis | Total sampled | Total positive | Right pelvic | Left pelvis |
| 76                              | 4+5 | 8.71   | 0                      | 0            | 0           | 0     | 0            | 0           | 11            | 0              | 0            | 0           |
| 65                              | 3+4 | 24.41  | 0                      | 0            | 0           | 0     | 0            | 0           | 19            | 0              | 0            | 0           |
| 63                              | 4+5 | 18.83  | 2                      | 1            | 1           | 1     | 0            | 0           | 23            | 0              | 0            | 0           |
| 66                              | 4+5 | 68.01  | 3                      | 2            | 1           | 4     | 3            | 1           | 21            | 5              | 5            | 0           |
| 68                              | 4+4 | 13.29  | 0                      | 0            | 0           | 0     | 0            | 0           | 15            | 0              | 0            | 0           |
| 46                              | 5+5 | 9.99   | 2                      | 1            | 1           | 2     | 1            | 1           | 21            | 3              | 2            | 1           |
| 59                              | 4+4 | 131.26 | 0                      | 0            | 0           | 2     | 1            | 1           | 27            | 2              | 1            | 1           |
| 56                              | 3+3 | 56.11  | 0                      | 0            | 0           | 2     | 1            | 1           | 18            | 1              | 0            | 1           |
| 70                              | 4+4 | 200.56 | 0                      | 0            | 0           | 0     | 0            | 0           | 16            | 0              | 0            | 0           |
| 56                              | 4+3 | 100.12 | 0                      | 0            | 0           | 2     | 1            | 1           | 28            | 3              | 1            | 2           |
| 59                              | 4+4 | 24.14  | 2                      | 2            | 0           | 6     | 2            | 4           | 29            | 11             | 7            | 4           |
| 57                              | 5+4 | 9.98   | 1                      | 0            | 1           | 2     | 1            | 1           | 15            | 2              | 1            | 1           |

HPE: Histopathology; MRI: Magnetic resonance imaging; PSMA: Prostate specific membrane antigen; PSA: Prostate-specific antigen

**Table 2: <sup>68</sup>Gallium-prostate specific membrane antigen-positron emission tomography-computed tomography detectability for number of patients with at least one histopathology positive lymph node**

|                                    | HPE positive |           | Total (%)   |
|------------------------------------|--------------|-----------|-------------|
|                                    | n (%)        | P (%)     |             |
| Total <sup>68</sup> Ga-PSMA-PET-CT |              |           |             |
| Negative                           | 4 (33.33)    | 0 (0.00)  | 4 (33.33)   |
| Positive                           | 1 (8.33)     | 7 (58.33) | 8 (66.67)   |
| Total                              | 5 (41.67)    | 7 (58.33) | 12 (100.00) |

HPE: Histopathology; <sup>68</sup>Ga-PSMA-PET-CT: <sup>68</sup>Gallium-prostate specific membrane antigen-positron emission tomography-computed tomography**Table 3: Magnetic resonance imaging detectability for number of patients with at least one histopathology positive lymph node**

|           | HPE positive |           | Total (%)   |
|-----------|--------------|-----------|-------------|
|           | n (%)        | P (%)     |             |
| Total MRI |              |           |             |
| Negative  | 4 (33.33)    | 3 (25.00) | 7 (58.33)   |
| Positive  | 1 (8.33)     | 4 (33.33) | 5 (41.67)   |
| Total     | 5 (41.67)    | 7 (58.33) | 12 (100.00) |

HPE: Histopathology; MRI: Magnetic resonance imaging

<sup>68</sup>Ga-PSMA PET-CT and MRI showed 21 and 10 positive lymph nodes, respectively. Their diagnostic value for number of lymph nodes detectability in comparison to HPE is given in Tables 4 and 5, respectively. <sup>68</sup>Ga-PSMA PET-CT and MRI diagnostic sensitivity, specificity, PPV, NPV, and accuracy for detection of lymph node metastasis in high risk case were 66.67%, 98.61%, 85.71%, 95.95%, 95.06%, and 25.93%, 98.61%, 70%, 91.42%, 90.53%, respectively. <sup>68</sup>Ga-PSMA PET-CT detected 18/27 (66.67%) true positive lymph nodes, whereas MRI detected 7/27 (25.93%) true positive lymph nodes. This difference of true positive lymph node detectability is significant on Chi-square test ( $P = 0.006$ ). All lymph node

seen on MRI ( $n = 7$ ) which were  $\geq 1$  cm were detected on <sup>68</sup>Ga-PSMA PET-CT [Figure 1]. However, the remaining sub-cm positive lymph nodes on HPE ( $n = 20$ , 74.08%), <sup>68</sup>GaPSMA PET-CT detected 11 (55%) of them [Figure 2].

We also compared by applying McNemar's test, the diagnostic sensitivities of <sup>68</sup>Ga-PSMA PET-CT and MRI for number of patients with at least one HPE positive lymph node [Table 6] and for overall lymph node detectability [Table 7].  $P$  value was statistically insignificant for number of patient detectability ( $P = 0.250$ ) between these two modalities but significant difference was seen for overall lymph nodal detection sensitivity ( $P = 0.001$ ).

For comparing overall detectability of these two imaging modalities for number of patients with at least one HPE positive lymph node [Figure 3] and for overall lymph node detection [Figure 4] by using area under the curve by applying comparison of independent receiver operating characteristic curve test, we found the statistically significant difference for overall lymph node detectability by <sup>68</sup>Ga-PSMA PET-CT ( $P = 0.0013$ ).

## Discussion

Lymph node dissection or sampling is a gold standard for lymph node staging in prostate cancer due to the size criteria limitation of conventional imaging modalities.<sup>[14]</sup> Using a minimum of size of 10 mm as threshold, the sensitivity of CT and MRI was found to be  $<40\%$ .<sup>[7,15]</sup> Abuzallouf *et al.* reported a series of 4264 patients in which 15.3% had positive lymph nodes on surgery, out of which only 2.5% had a positive CT scan. The median estimated sensitivity, specificity, NPV, and PPV were 7%, 100%, 85%, and 100%, respectively.<sup>[16]</sup>

**Table 4:  $^{68}\text{Ga}$ -prostate specific membrane antigen-positron emission tomography-computed tomography detectability for lymph node metastasis in comparison to histopathology**

|                               | HPE         |            | Total (%)    |
|-------------------------------|-------------|------------|--------------|
|                               | n (%)       | P (%)      |              |
| $^{68}\text{Ga}$ -PSMA-PET-CT |             |            |              |
| Negative                      | 213 (87.65) | 9 (3.70)   | 222 (91.36)  |
| Positive                      | 3 (1.23)    | 18 (7.41)  | 21 (8.64)    |
| Total                         | 216 (88.89) | 27 (11.11) | 243 (100.00) |

HPE: Histopathology;  $^{68}\text{Ga}$ -PSMA-PET-CT:  $^{68}\text{Ga}$ -prostate specific membrane antigen-positron emission tomography-computed tomography

**Table 5: Magnetic resonance imaging detectability for lymph node metastasis in comparison to histopathology**

|          | HPE         |            | Total (%)    |
|----------|-------------|------------|--------------|
|          | n (%)       | P (%)      |              |
| MRI      |             |            |              |
| Negative | 213 (87.65) | 20 (8.23)  | 233 (95.88)  |
| Positive | 3 (1.23)    | 7 (2.88)   | 10 (4.12)    |
| Total    | 216 (88.89) | 27 (11.11) | 243 (100.00) |

HPE: Histopathology; MRI: Magnetic resonance imaging

**Table 6:  $^{68}\text{Ga}$ -prostate specific membrane antigen-positron emission tomography-computed tomography and magnetic resonance imaging comparison of sensitivities for number of patients with at least one histopathology positive lymph node (McNemar's test)**

|          | Total $^{68}\text{Ga}$ -PSMA-PET-CT, P (%) | Total (%)  | P     | Difference (%) |
|----------|--|------------|-------|----------------|
| MRI      |  |            | 0.250 | 42.86          |
| Negative | 3 (42.86)                                  | 3 (42.86)  |       |                |
| Positive | 4 (57.14)                                  | 4 (57.14)  |       |                |
| Total    | 7 (100.00)                                 | 7 (100.00) |       |                |

MRI: Magnetic resonance imaging;  $^{68}\text{Ga}$ -PSMA-PET-CT:  $^{68}\text{Ga}$ -prostate specific membrane antigen-positron emission tomography-computed tomography

**Table 7:  $^{68}\text{Ga}$ -prostate specific membrane antigen-positron emission tomography-computed tomography and magnetic resonance imaging comparison of sensitivities for histopathology positive lymph node (McNemar's test)**

|          | Total $^{68}\text{Ga}$ -PSMA-PET-CT, n (%) | Total (%)  | P     | Difference (%) |
|----------|--|------------|-------|----------------|
| MRI      |  |            | 0.001 | 40.75          |
| Negative | 9 (33.33)                                  | 11 (40.74) |       | 20 (74.07)     |
| Positive | 0 (0.00)                                   | 7 (25.93)  |       | 7 (25.93)      |
| Total    | 9 (33.33)                                  | 18 (66.67) |       | 27 (100.00)    |

HPE: Histopathology; MRI: Magnetic resonance imaging;  $^{68}\text{Ga}$ -PSMA-PET-CT:  $^{68}\text{Ga}$ -prostate specific membrane antigen-positron emission tomography-computed tomography

2-fluoro-2-deoxyglucose ( $^{18}\text{F}$ ) PET-CT has also not been very effective due to the known low-glucose utilization

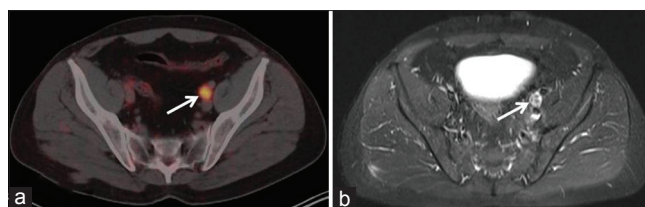


**Figure 1:** Axial fused  $^{68}\text{Ga}$ -prostate specific membrane antigen-positron emission tomography-computed tomography (a) and T2W turbo inversion recovery magnitude sequence, (b) enlarged prostate specific membrane antigen positive left pelvic lymph node (white arrow)

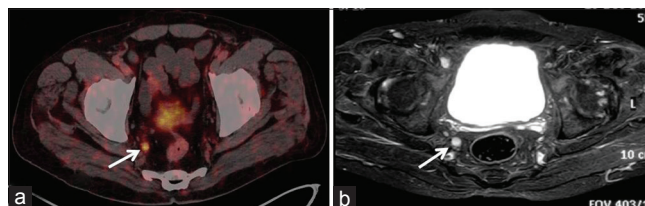


**Figure 2:** Axial fused  $^{68}\text{Ga}$ -prostate specific membrane antigen-positron emission tomography-computed tomography (a) and T2W turbo inversion recovery magnitude sequence, (b) sub centimeter prostate specific membrane antigen positive right pelvic lymph node (white arrow)

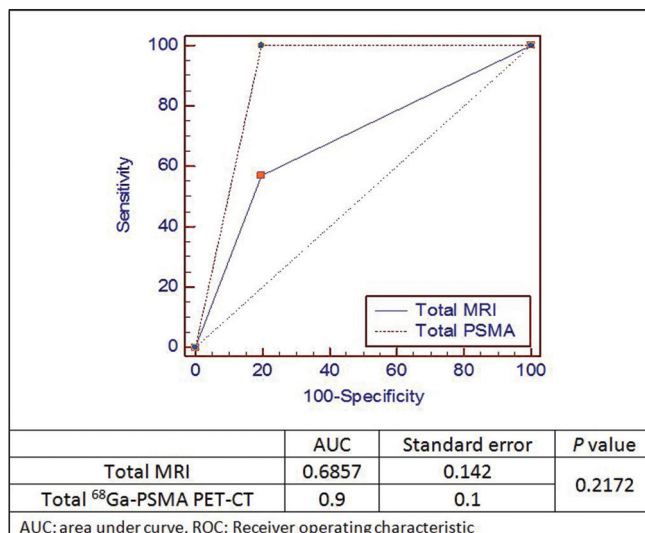


**Figure 3:**  $^{68}\text{Ga}$ -prostate specific membrane antigen-positron emission tomography-computed tomography and magnetic resonance imaging comparison of area under the curve using comparison of independent receiver operating characteristic curve test for number of patients with at least one histopathology positive lymph node

of the well differentiated prostate cancer.<sup>[17]</sup> ePLND being an invasive procedure associated with morbidities should not be used as a staging procedure and should only be used as a therapeutic procedure when indicated.<sup>[18,19]</sup> Therefore, there is certainly a need for a sensitive imaging procedure, which can predict with a reasonable certainty about the nodal involvement for an accurate surgical planning.



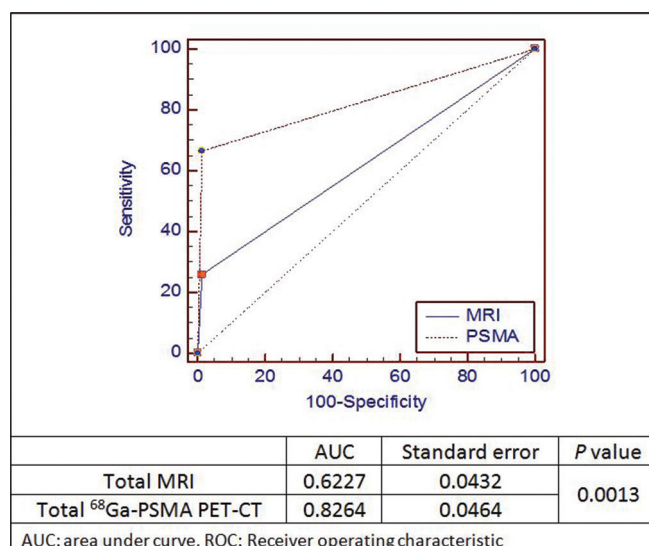


**Figure 4:** <sup>68</sup>Gallium-prostate specific membrane antigen-positron emission tomography-computed tomography positron emission tomography-computed tomography and magnetic resonance imaging comparison of area under the curve using comparison of independent receiver operating characteristic curve test for histopathology positive lymph node

In current times, molecular targeting with specific and near specific tracers has opened a new horizon for imaging prostate cancer. Initially, <sup>11</sup>C-choline followed by <sup>18</sup>F-choline was used for prostate cancer imaging. Evangelista *et al.* did a literature review and meta-analysis of choline PET-CT for lymph node involvement identification in intermediate to high-risk prostate cancer and reported pooled sensitivity 49.2% (95% confidence interval [CI], 39.9–58.4), and pooled specificity 95% (95% CI, 92–97.1).<sup>[20]</sup> PSA and prostate specific acid phosphatase could not live up to the expectations for imaging due to their secretory nature.<sup>[21]</sup> PSMA is a type II membrane glycoprotein consisting of 750 amino acids (100–120 kDa), with a 19 amino acid intracellular component, a 24 amino acid transmembrane segment, and a large 707 amino acid extracellular component.<sup>[22]</sup> Extracellular portion of PSMA exhibits folate hydrolase/glutamate carboxypeptidase II enzymatic activity. However, its precise role in *in vivo* has not yet been fully elucidated.<sup>[23]</sup> *In vitro* its folate hydrolase activity has been associated with prostatic carcinogenesis.<sup>[24]</sup> Its expression is also directly proportional to Gleason score, metastasis, and hormone resistance in prostate cancer. PSMA is also expressed in salivary glands, duodenal mucosa, subset of proximal renal tubular cells, and subpopulation of neuroendocrine cells in colonic crypts small intestine.<sup>[25]</sup> In last several years, a number of small molecules with PSMA enzyme inhibitor property have been developed. Small molecule inhibitor <sup>68</sup>Ga-DKFZ-11 (<sup>68</sup>Ga-PSMA) has been shown to be a novel radiotracer with high-cell uptake and prolonged retention after internalization for prostate cancer.<sup>[26,27]</sup>

There are very few studies in the literature dealing with the role of PSMA PET-CT in staging of prostate cancer. Most of the literature pertain to recurrence of castration resistant prostate cancer. Afshar-Oromieh *et al.* studied 42 recurrent prostate cancer patients and compared the positive lymph nodes in PSMA PET-CT with biopsy or surgery.<sup>[12]</sup> The diagnostic sensitivity and specificity was found to be 76.6% and 100%, respectively. These findings were slightly better than our results of sensitivity and specificities 66.67% and 98.61%, respectively; however, this difference is not statistically significant ( $P = 0.4027$ ). This slight difference may be due to interobserver variability or less volume of disease in recurrent case, hence more tracer availability.

On the other hand, Budäus *et al.* recently published his initial experience of <sup>68</sup>Ga-PSMA PET-CT imaging in high-risk prostate cancer patients before radical prostatectomy.<sup>[28]</sup> He found an overall sensitivity, specificity, PPV and NPV of <sup>68</sup>Ga-PSMA PET-CT for lymph node metastasis detection was 33.3%, 100%, 100%, and 69.2%, respectively, which was lower than our findings. Patient selection criteria may be one of the factors for this difference. In his study, the disease prevalence was lower both by number of positive patient (40.0% vs. 58.33%) and total number of positive lymph nodes (8.7% vs. 11.11%) and this could be the major factor for these differences. Moreover, in his study, <sup>68</sup>Ga-PSMA PET-CT was performed in multiple institutes nationwide, so differences in opinion among experts may not be ruled out despite high-volume imaging. In addition, criteria for positive <sup>68</sup>Ga-PSMA PET-CT for lymph node was also not mentioned.

The major limitation of our study is the small number of patients mostly due to a very specific patient's selection criteria. In prostate cancer, during staging, most of the lymph nodes were <8 mm in size,<sup>[29]</sup> and therefore, there is bound fallacies in a technique which uses only size criteria for interpretation.

## Conclusion

Although <sup>68</sup>Ga-PSMA PET-CT imaging is more used in recurrent prostate cancer to assess the disease site and volume, our initial experience has shown that PSMA PET-CT is a very promising tracer for N staging in the initial evaluation of prostate cancer. It has the potential to have an overall impact in the patient's initial management by either up-staging or down-staging the disease.

**Financial support and sponsorship**  
Nil.

## Conflicts of interest

The authors declare no conflicts of interest.

## References

- Jain S, Saxena S, Kumar A. Epidemiology of prostate cancer in India. *Meta Gene* 2014;2:596-605.
- Edge SB, Byrd DR, Compton CC, Fritz AG, Greene FL, Trotti A, editors. *AJCC Cancer Staging Manual*. 7<sup>th</sup> ed. New York, NY: Springer; 2010. p. 457-68.
- Heidenreich A, Bastian PJ, Bellmunt J, Bolla M, Joniau S, van der Kwast T, *et al.* EAU guidelines on prostate cancer. Part 1: Screening, diagnosis, and local treatment with curative intent-update 2013. *Eur Urol* 2014;65:124-37.
- Partin AW, Mangold LA, Lamm DM, Walsh PC, Epstein JI, Pearson JD. Contemporary update of prostate cancer staging nomograms (Partin Tables) for the new millennium. *Urology* 2001;58:843-8.
- Eifler JB, Feng Z, Lin BM, Partin MT, Humphreys EB, Han M, *et al.* An updated prostate cancer staging nomogram (Partin tables) based on cases from 2006 to 2011. *BJU Int* 2013;111:22-9.
- Cagiannos I, Karakiewicz P, Eastham JA, Ohori M, Rabbani F, Gerigk C, *et al.* A preoperative nomogram identifying decreased risk of positive pelvic lymph nodes in patients with prostate cancer. *J Urol* 2003;170:1798-803.
- Hövels AM, Heesakkers RA, Adang EM, Jager GJ, Strum S, Hoogveen YL, *et al.* The diagnostic accuracy of CT and MRI in the staging of pelvic lymph nodes in patients with prostate cancer: A meta-analysis. *Clin Radiol* 2008;63:387-95.
- Jager GJ, Barentsz JO, Oosterhof GO, Witjes JA, Ruijs SJ. Pelvic adenopathy in prostatic and urinary bladder carcinoma: MR imaging with a three-dimensional T1-weighted magnetization-prepared-rapid gradient-echo sequence. *AJR Am J Roentgenol* 1996;167:1503-7.
- Conti M. New prospects for PET in prostate cancer imaging: A physicist's viewpoint. *EJNMMI Phys* 2014;1:11.
- Wright GL Jr., Haley C, Beckett ML, Schellhammer PF. Expression of prostate-specific membrane antigen in normal, benign, and malignant prostate tissues. *Urol Oncol* 1995;1:18-28.
- Perner S, Hofer MD, Kim R, Shah RB, Li H, Möller P, *et al.* Prostate-specific membrane antigen expression as a predictor of prostate cancer progression. *Hum Pathol* 2007;38:696-701.
- Afshar-Oromieh A, Avtzi E, Giesel FL, Holland-Letz T, Linhart HG, Eder M, *et al.* The diagnostic value of PET/CT imaging with the (68) Ga-labelled PSMA ligand HBED-CC in the diagnosis of recurrent prostate cancer. *Eur J Nucl Med Mol Imaging* 2015;42:197-209.
- Eiber M, Maurer T, Souvatzoglou M, Beer AJ, Ruffani A, Haller B, *et al.* Evaluation of hybrid <sup>68</sup>Ga-PSMA ligand PET/CT in 248 patients with biochemical recurrence after radical prostatectomy. *J Nucl Med* 2015;56:668-74.
- Mottet N, Bellmunt J, Briers E, van den Bergh RC, Bolla M, van Casteren NJ, *et al.* European Association of Urology Guidelines on Prostate Cancer; 2015. p. 28-29. Available from: <http://www.uroweb.org/guideline/prostate-cancer/>. [Last accessed on 2016 Apr 15].
- Hricak H, Doms GC, Jeffrey RB, Avallone A, Jacobs D, Benton WK, *et al.* Prostatic carcinoma: Staging by clinical assessment, CT, and MR imaging. *Radiology* 1987;162:331-6.
- Abuzallouf S, Dayes I, Lukka H. Baseline staging of newly diagnosed prostate cancer: A summary of the literature. *J Urol* 2004;171(6 Pt 1):2122-7.
- Jadvar H. Prostate cancer: PET with 18F-FDG, 18F-or 11C-acetate, and 18F-or 11C-choline. *J Nucl Med* 2011;52:81-9.
- Hutterer GC, Briganti A, Chun FK, Gallina A, Rigatti P, Montorsi F, *et al.* The evolution of staging of lymph node metastases in clinically localized prostate cancer. *EAU EBU Update Ser* 2007;5:153-62.
- Bivalacqua TJ, Pierorazio PM, Gorin MA, Allaf ME, Carter HB, Walsh PC. Anatomic extent of pelvic lymph node dissection: Impact on long-term cancer-specific outcomes in men with positive lymph nodes at time of radical prostatectomy. *Urology* 2013;82:653-8.
- Evangelista L, Guttilla A, Zattoni F, Muzzio PC, Zattoni F. Utility of choline positron emission tomography/computed tomography for lymph node involvement identification in intermediate- to high-risk prostate cancer: A systematic literature review and meta-analysis. *Eur Urol* 2013;63:1040-8.
- Tagawa ST, Beltran H, Vallabhajosula S, Goldsmith SJ, Osborne J, Matulich D, *et al.* Anti-prostate-specific membrane antigen-based radioimmunotherapy for prostate cancer. *Cancer* 2010;116 4 Suppl:1075-83.
- Mease RC, Foss CA, Pomper MG. PET imaging in prostate cancer: Focus on prostate-specific membrane antigen. *Curr Top Med Chem* 2013;13:951-62.
- Barinka C, Rojas C, Slusher B, Pomper M. Glutamate carboxypeptidase II in diagnosis and treatment of neurologic disorders and prostate cancer. *Curr Med Chem* 2012;19:856-70.
- Yao V, Parwani A, Maier C, Heston WD, Bacich DJ. Moderate expression of prostate-specific membrane antigen, a tissue differentiation antigen and folate hydrolase, facilitates prostate carcinogenesis. *Cancer Res* 2008;68:9070-7.
- Silver DA, Pellicer I, Fair WR, Heston WD, Cordon-Cardo C. Prostate-specific membrane antigen expression in normal and malignant human tissues. *Clin Cancer Res* 1997;3:81-5.
- Eder M, Schäfer M, Bauder-Wüst U, Haberkorn U, Eisenhut M, Kopka K. Preclinical evaluation of a bispecific low-molecular heterodimer targeting both PSMA and GRPR for improved PET imaging and therapy of prostate cancer. *Prostate* 2014;74:659-68.
- Afshar-Oromieh A, Malcher A, Eder M, Eisenhut M, Linhart HG, Hadaschik BA, *et al.* PET imaging with a [68Ga] gallium-labelled PSMA ligand for the diagnosis of prostate cancer: Biodistribution in humans and first evaluation of tumour lesions. *Eur J Nucl Med Mol Imaging* 2013;40:486-95.
- Budäus L, Leyh-Bannurah SR, Salomon G, Michl U, Heinzer H, Huland H, *et al.* Initial experience of (68) Ga-PSMA PET/CT imaging in high-risk prostate cancer patients prior to radical prostatectomy. *Eur Urol* 2016;69:393-6.
- Li L, Wang L, Feng Z, Hu Z, Wang G, Yuan X, *et al.* Prostate cancer magnetic resonance imaging (MRI): Multidisciplinary standpoint. *Quant Imaging Med Surg* 2013;3:100-12.